Keplerian disks and outflows around binary post-AGB stars

I. Gallardo Cava [1, 2]
i.gallardocava@oan.es

V. Bujarrabal [1], J. Alcolea [1], M. Gómez-Garrido [1, 2], A. Castro-Carrizo [3], H. Van Winckel [4], and M. Santander-García [1]

[1] OAN-IGN (Spain), [2] Universidad Complutense de Madrid (Spain), [2] IRAM (France), and [4] KU Leuven (Belgium)

1. Introduction

Most of the pre-planetary (or protoplanetary) and planetary nebulae (pPNe and PNe) show fast bipolar outflows (30-100 km s^{-1}) with clear axial symmetry. These outflows are responsible for a good fraction of the total mass. AGB stars, present spherical circumstellar envelopes. The spectacular evolution from AGB circumstellar envelopes to post-AGB nebulae takes place in a very short time (~1000 yr). The accepted scenario to explain this evolution implies that ma-terial is accreted by a companion from a rotating disk, followed by the launching of very fast jets, in a process similar to that in protostars [4, 14].

There is a class of **binary post-AGB stars that systematically show evidence of the presence of disks** [5, 11, 8, 14]. All of them present a remarkable near-infrared (NIR) excess and the narrow CO line profiles characteristic of rotating disks. Their spectral energy distributions (SEDs) reveal the presence of hot dust close to the stellar system, and its disk-like shape has been confirmed by interferometric IR data [8, 9]. These disks must be stable structures, because their IR spectra reveal the presence of highly processed grains [13], see Fig. 1. Observations of ^{12}CO and ^{13}CO in the J=2−1 and J=1−0 lines have been well analyzed in sources with such a NIR excess [5] and they show line profiles formed by a narrow single peak and relatively wide wings or a narrow CO line profile with strong wings. (see Fig. 2) These results indicate that the CO emission lines of our sources come from Keplerian disks.

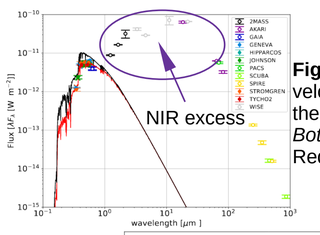

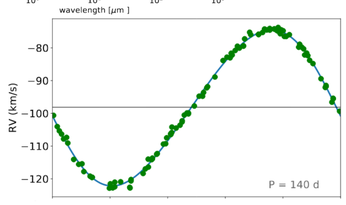

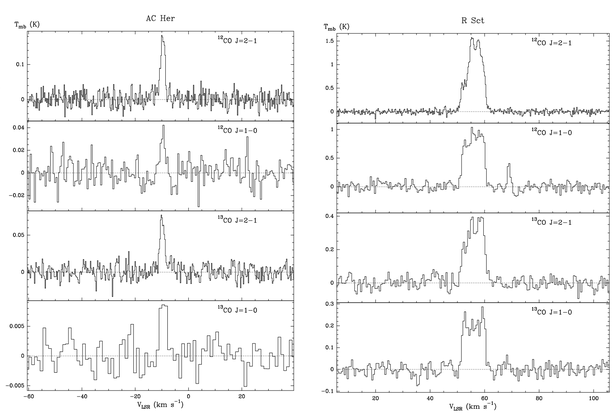

Fig. 1: *Top*: Radial velocity curve for the Red Rectangle. *Bottom*: SED of the Red Rectangle.

Fig. 2: *Left*: CO line profiles of AC Her. They present narrow component and wide wings. This kind of emission is characteristic of rotating disks. *Right*: R Sct present composite CO line profiles including a narrow component which very probably represents emission from the rotating disk. This emission represents a rotating disk surrounded by an extended and prominent outflow.

2. Millimeter interferometric maps of CO lines and models

The study of Keplerian disks around post-AGB stars requires high angular- and spectral-resolution observations because of the relative small size of the disks. There is another structure surrounding the disk and presents expansion velocity. There are seven well studied sources in mm-wave interferometric CO lines: Red Rectangle [3], IW Car [4], IRAS 08544−4431 [5], AC Her [6], 89 Her [6], IRAS 19125+0343 [6], and R Sct [6]. According to the observations, **we can distinguish between sources in which the disk is the dominant component** (such as AC Her, see Figs. 3 and 4 *Top*) **and sources dominated by the outflow** (such as R Sct, see Figs 7 and 8).

Our models consist of a rotating disk surrounded by an outer outflow that can present different shapes (ellipsoidal, hourglass, etc). We consider potential laws for the density and rotational temperature. We assume Keplerian rotation in the disk and radial expansion velocity in the outflow. **Our code produces results that can be quantitatively compared to observations** (see Figs. 4 *Bottom* and 5).

Our predictions reveals that **there two subclass of binary post-AGB stars** with NIR excess: **the disk- and the outflow-dominated nebulae**. The disk-dominated sources contain most of the material of the nebula located in the disk (~90%). On the contrary, the outflow-dominated present massive outflows, even more massive than their disks (~75%). These outflows are mostly composed of cold gas [6].

AC Herculis: disk-dominated

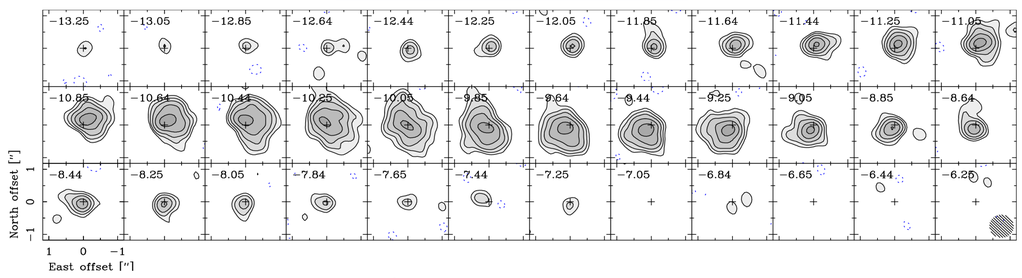

Fig. 3: NOEMA maps per velocity channel of ^{12}COJ=2−1 emission from AC Her. The beam size (HPBW) is 0.″35×0.″35. The contour spacingis logarithmic: ±9, 18, 36, 76, and 144 mJy beam^{-1} with a maximum emission peak of 230 mJy beam^{-1}.

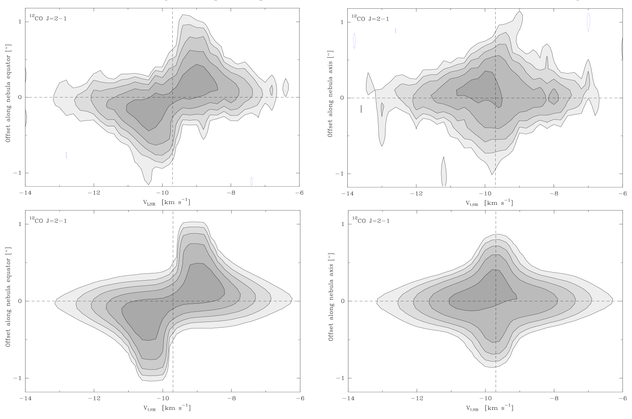

Fig. 4: *Top left*: Position-velocity diagram from our NOEMA maps of ^{12}CO J=2−1 in AC Her along the direction PA=136.1º, corresponding to the nebula equator. *Top right*: Same as in *Top left* but along the perpendicular direction PA=46.1º. *Bottom left* and *Bottom right*: same as in *Top left* and *Top right*, but for synthetic PV diagrams.

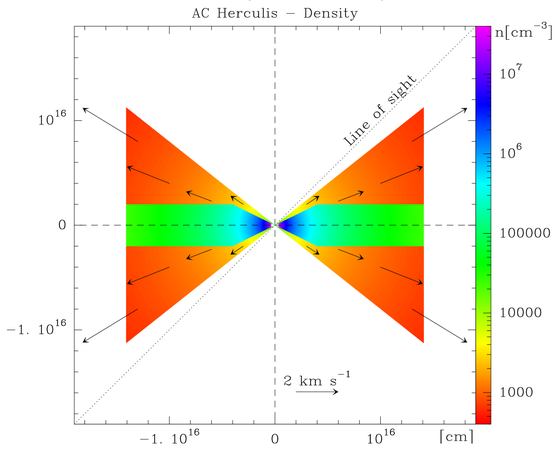

Fig. 5: Structure and distribution of the density of our best-fit model for the disk and outflow of AC Her. The Keplerian disk presents density values ≥10^{5}cm^{-3}. The expansion velocity is represented with arrows.

R Scuti: outflow-dominated

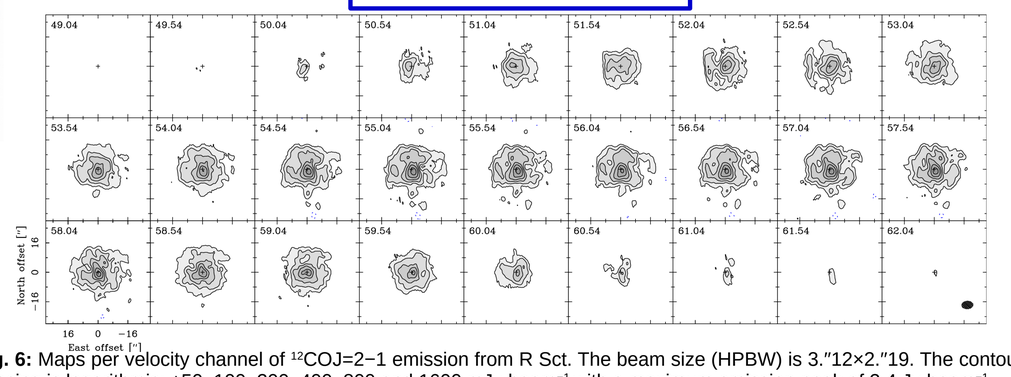

Fig. 6: Maps per velocity channel of ^{12}COJ=2−1 emission from R Sct. The beam size (HPBW) is 3.″12×2.″19. The contour spacing is logarithmic: ±50, 100, 200, 400, 800 and 1600 mJy beam^{-1} with a maximum emission peak of 2.4 Jy beam^{-1}.

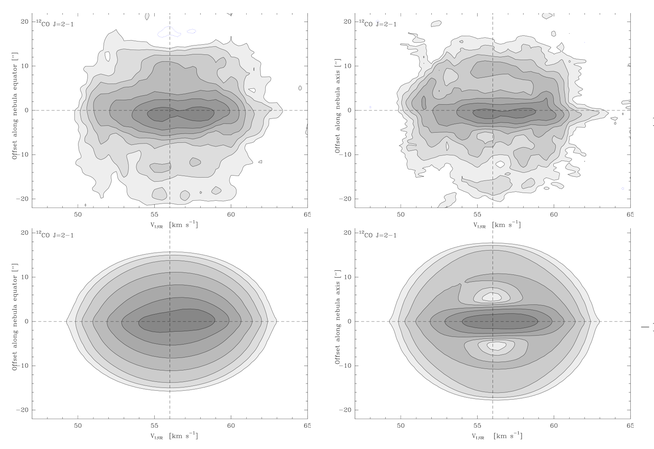

Fig. 7: *Top left*: Position-velocity diagram from our NOEMA maps of ^{12}COJ=2−1 in R Sct along the direction PA=0º, corresponding to the nebula equator. *Top right*: Same as in *Left* but along the perpendicular direction PA=90º. *Bottom left* and *Bottom right*: same as in *Top left* and *Top right*, but for synthetic PV diagrams.

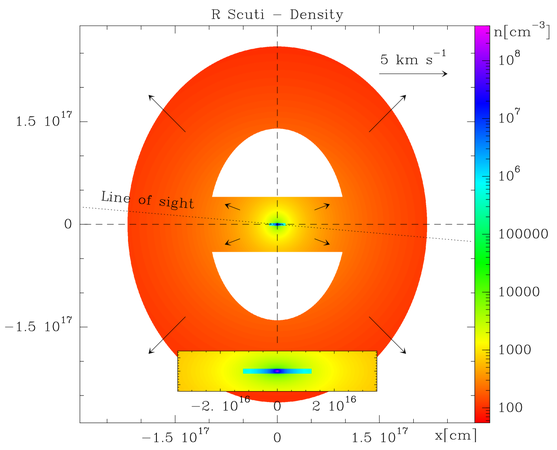

Fig. 8: Structure and distribution of the density of our best-fit model for the disk and outflow of R Sct. The lower inset shows a zoom into the inner region of the nebula where the Keplerian disk presents density values ≥ 10^{6}cm^{-3}. The expansion velocity is represented with arrows.

3. The chemistry of nebulae around binary post-AGB stars

We also present a very deep single-dish radio molecular survey in the 1.3, 2, 3, 7, and 13 mm bands in nebulae around binary post-AGB stars [7]. We confirm the relatively **low molecular content in nebulae around binary post-AGB stars**, as their molecular lines are weaker compared with AGB stars (see Fig. 9 *Left*). This fact is very significant in those sources in which the Keplerian disk is the dominant component of the nebula.

Compared with the IR fluxes (see Fig. 9 *Right top*), **the ^{12}CO emission is relatively low with respect to the levels exhibited by AGB stars**. We find again two subclasses in our sample. Those sources in which the Keplerian disk dominates the nebula tend to present a clearly lower relative intensity of ^{12}CO compared to the outflow-dominated ones. On the contrary, we do not see this effect in ^{13}CO emission, which seems to be relatively intense compared with ^{12}CO, and comparable with respect to AGB stars.

Integrated intensities are larger for O-rich than for C-rich objects when an O-bearing molecule is compared with a C-bearing one (see Fig. 9 *Bottom right*). Our results are compared with CSEs around AGB stars, which are deeply studied objects and are prototypical media rich in molecules. 89 Her presents a O/C < 1 chemistry. On the contrary, AI CMi , IRAS 20056+1834, and R Sct present a O/C > 1 chemistry. The chemistry of the Red Rectangle could be uncertain, but we have also classified this source as O-rich.

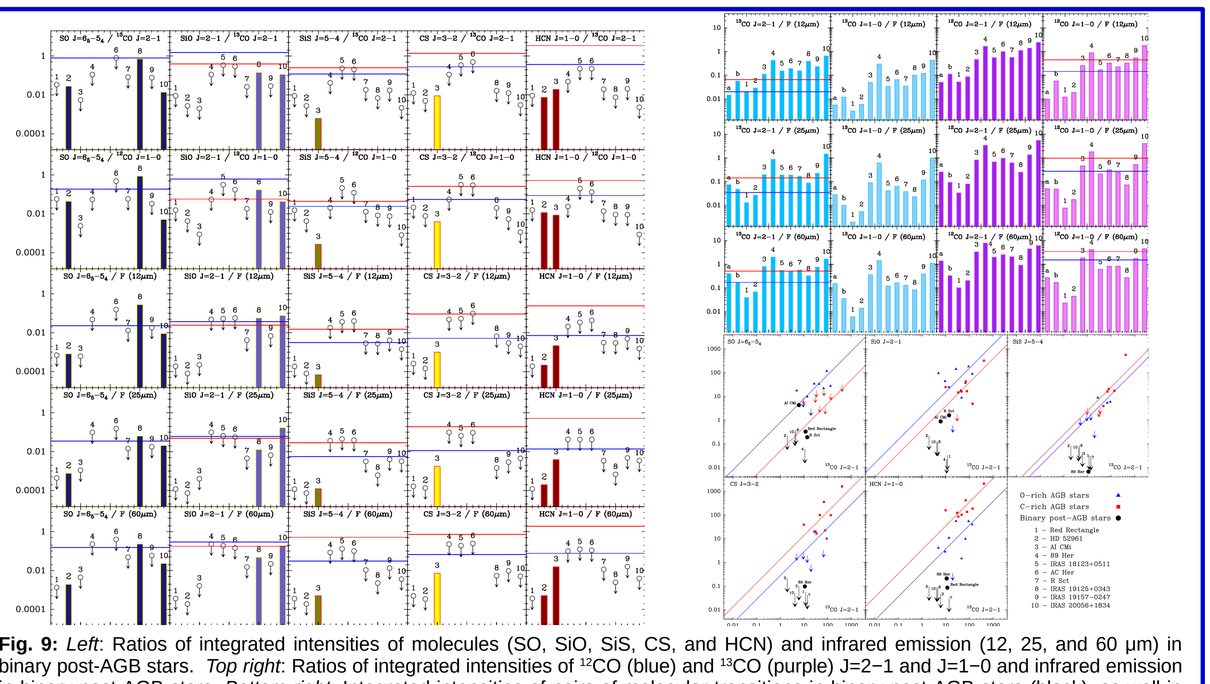

Fig. 9: *Left*: Ratios of integrated intensities of molecules (SO, SiO, SiS, CS, and HCN) and infrared emission (12, 25, and 60 μm) in binary post-AGB stars. *Top right*: Ratios of integrated intensities of ^{12}CO (blue) and ^{13}CO (purple) J=2−1 and J=1−0 and infrared emission in binary post-AGB stars. *Bottom right*: Integrated intensities of pairs of molecular transitions in binary post-AGB stars (black), as well in O- and C-rich stars (blue and red). X and Y axes represent the integrated intensities of the observed transitions in logarithmic scale and units of Jy km s^{-1}. Upper limits are always represented with empty circles. Blue and red lines always represent the averaged values for O- and C-rich AGB CSEs. Sources are always ordered by increasing outflow dominance and enumerated as follows: a - HR 4049, b - DY Ori, 1 - AC Her, 2 - Red Rectangle, 3 - 89 Her, 4 - HD 52961, 5 - IRAS 19157−0257, 6 - IRAS 18123+0511, 7 - IRAS 19125+0343, 8 - AI CMi, 9 - IRAS 20056+1834, and 10 - R Sct.

4. Conclusions

Our mm-wave observations and models allow us to conclude that there are two subclasses of binary post-AGB stars: the disk- (Red Rectangle, AC Her, IW Car, and IRAS 08544−4431) and the outflow-dominated nebulae (89 Herculis, IRAS 19125+0343, R Sct). These present massive outflows, mostly composed of cold gas, even more massive than their disks.

We present the first single-dish molecular survey of mm-wave lines in nebulae around binary post-AGB stars. We confirm their relatively low molecular content. The study of their chemisty allows us to classify nebulae around the Red Rectangle, AI CMi, R Sct, and IRAS 20056+1834 as O-rich, while that of 89 Her is C-rich.

References. [1] Blackman, E. G. & Lucchini, S. 2014, MNRAS, 440, L16; [2] Bujarrabal, V., Alcolea, J., Van Winckel, H., Santander-García, M., & Castro-Carrizo, A. 2013a, A&A, 557, A104; [3] Bujarrabal, V., Castro-Carrizo, A., Alcolea, J., et al. 2016, A&A, 593, A92; [4] Bujarrabal, V., Castro-Carrizo, A., Alcolea, J., et al. 2017, A&A, 597, L5, [5] Bujarrabal, V., Castro-Carrizo, A., Van Winckel, H., et al. 2018, A&A, 614, A58, [6] Gallardo Cava, I., Gómez-Garrido, M., Bujarrabal, V., et al. 2021, A&A, 648,A93, [7] Gallardo Cava, I., Bujarrabal, V., Alcolea, J., Gómez-Garrido, M., and Santander-García, M., A&A (submitted), [8] Hillen, M., Van Winckel, H., Menu, J., et al. 2017, A&A, 599, A41, [9] Kluska, J., Van Winckel, H., Hillen, M., et al. 2019, A&A, 631, A108, [10] Oomen, G.-M., Van Winckel, H., Pols, O., et al. 2018, A&A, 620, A85, [11] de Ruyter, S., van Winckel, H., Maas, T., et al. 2006, A&A, 448, 641, [12] Sahai, R., Claussen, M. J., Schnee, S., Morris, M. R., & Sánchez Contreras, C.2011, ApJ, 739, L3, [13] Soker, N. 2002, ApJ, 568, 726, [14] Van Winckel, H. 2003, ARA&A, 41, 391

Acknowledgements. This work is based on observations of IRAM telescopes. IRAM is supported by INSU/CNRS (France), MPG (Germany), and IGN (Spain). This work is part of the AxiN and EVENTs/NEBULEA WEB research programs supported by Spanish AEI grants AYA 2016-78994-P and PID2019-105203GB-C21. Iván Gallardo Cava acknowledges Spanish MICIN the funding support of BES2017-080616.